



Optimizing Chemical Reactor Performance Using Frustum Geometry: A Comparative Analysis of Gas and Liquid Phase Reactions

Bubakr M. M. Alshukri¹, Ali Hamed Elhudhiry², Abdalla EL-Twaty² and Isam Salem²

¹Sarir Oil Operations, Benghazi, Libya

²University of Benghazi, Benghazi, Libya

Corresponding Author: Ali.elhudhiry@uob.edu.ly

ARTICLE INFOR

Article history:

Received 18 March 2025

Revised 28 March 2025

Accepted 2 April 2025

Available online

15 May 2025

ABSTRACT

This study investigates the impact of reactor geometry on chemical reaction efficiency, focusing on the application of frustum-shaped reactors compared to conventional cylindrical designs. The research examines the performance of gas-phase and liquid-phase reactions, evaluating conversion rates, pressure distribution, and overall reaction effectiveness. The results indicate that while frustum geometry enhances conversion in gas-phase reactions due to its unique pressure distribution, its impact on liquid-phase reactions remains minimal. These findings provide valuable insights for optimizing industrial reactor design and improving process efficiency.

2025 Sirte University, All rights are reserved

Keywords: Frustum, Reactor Geometry, Pressure Distribution, Reactor Configurations.

1. Introduction

The design and optimization of chemical reactors play a crucial role in maximizing efficiency, improving product yields, and minimizing operational costs in the chemical and petroleum industries. Researchers have long dedicated efforts to identifying reactor configurations that enhance the production of desired products. Various types of reactors and different modes of operation have been developed over the years to optimize reaction performance under diverse industrial conditions.

(Fogler, 2016) Traditionally, reactor designs have been categorized based on their geometry and the flow pattern of the reactants. Some of the most common reactor configurations include:

- Axial-flow tubular reactors
- Radial-flow tubular reactors
- Axial-flow spherical reactors
- Radial-flow spherical reactors

Each of these reactor designs presents distinct advantages and challenges. Tubular reactors, for example, provide efficient heat transfer and are commonly used in large-scale industrial processes, while spherical reactors allow for enhanced mixing and uniform temperature distribution. The evolution of reactor geometries has been driven by the need to balance heat management, pressure drop, and catalyst utilization to achieve optimal reaction conditions.

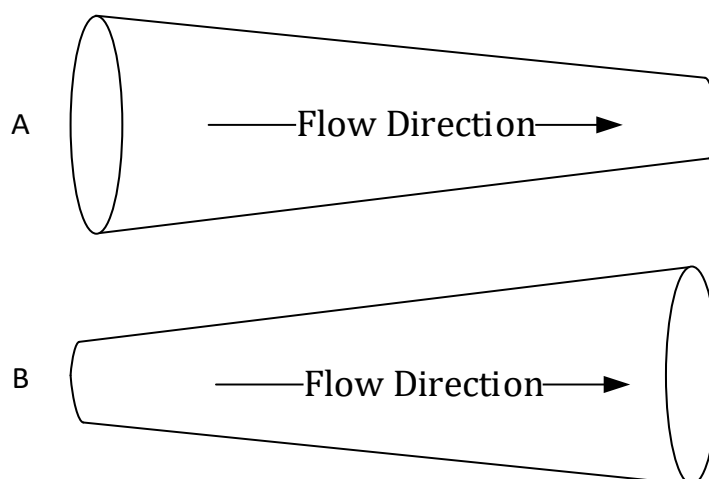


Figure 1 Frustum shape which will be use as a reactor (B) will be called a positive frustum (A) will be called a negative frustum

In recent years, novel reactor configurations have emerged to address limitations in conventional designs. One such innovation is the introduction of frustum-shaped reactors, which offer unique advantages over traditional geometries. The frustum design, characterized by its truncated cone shape, introduces gradual variations in pressure and flow dynamics that can positively impact reaction kinetics. Unlike conventional reactor geometries that rely on modifying feed conditions or increasing catalyst volume to enhance conversion rates, the frustum reactor leverages its shape to achieve improved conversion without altering these parameters. (Smith et al., 2005)

This study explores the potential of frustum reactor geometry in optimizing chemical conversion processes. By analysing the impact of the frustum design on reaction efficiency, catalyst distribution, and pressure dynamics, this research aims to demonstrate how reactor geometry can be strategically utilized to improve performance without requiring additional feedstock or catalyst volume (Baerns, 2004). The findings of this study contribute to the ongoing advancements in reactor design and provide valuable insights for industrial applications seeking to enhance process efficiency while maintaining cost-effectiveness.

2. Aim of the Study

This study aims to investigate the impact of applying frustum reactor geometry on the conversion efficiency of different chemical reactions. By examining three distinct reaction types—a liquid-phase isomerization of normal butane, the gas-phase oxidation of ethylene with air (synthesis reaction), and the gas-phase dehydrogenation of paraffins to olefins—this research seeks to determine whether frustum-shaped reactors can enhance reaction performance without requiring changes in feed conditions or catalyst quantity. The goal is to assess how pressure distribution, catalyst arrangement, and residence time variations influence reaction kinetics and conversion rates, ultimately providing insights into the feasibility of implementing frustum reactors in industrial applications.

3. Problem Statement

In industrial chemical processes, reactor design plays a critical role in optimizing conversion rates, selectivity, and overall process efficiency. Conventional reactor configurations, such as tubular and spherical reactors, have been extensively studied and implemented. However, they often require modifications in operating conditions, catalyst load, or reactor size to achieve optimal performance.

The challenge lies in improving reaction conversion without increasing operational costs or altering fundamental process conditions. Recent studies suggest that reactor geometry significantly influences reaction kinetics, particularly in terms of pressure drop, catalyst distribution, and heat transfer. The frustum geometry presents a unique opportunity to enhance conversion efficiency by leveraging its shape-induced pressure and flow characteristics. (Satterfield, 1991)

Despite its theoretical advantages, limited research has explored the practical implications of frustum reactor designs across different reaction types. This study seeks to bridge that gap by analysing its effects on both gas-phase and liquid-phase

reactions, aiming to provide a deeper understanding of how reactor geometry can be optimized for industrial-scale applications. (Yagi & Kunii, 1971).

4. Literature Review

4.1 *Evolution of Reactor Design*

The development of chemical reactor configurations has been a subject of extensive research due to its direct impact on reaction efficiency, selectivity, and industrial feasibility. Researchers have continuously explored different reactor geometries to enhance process performance by optimizing heat transfer, pressure distribution, and catalyst utilization.

Traditionally, reactors have been categorized based on their flow patterns and geometry:

- **Axial-Flow Tubular Reactors:** These are widely used for gas-phase reactions where plug flow behavior is required. The uniform flow profile ensures predictable residence time, which is advantageous for high-selectivity reactions (Fogler, 2016).
- **Radial-Flow Tubular Reactors:** This design is commonly employed in catalytic reforming due to its ability to reduce pressure drop while maximizing contact with the catalyst.
- **Axial-Flow Spherical Reactors:** These reactors provide enhanced temperature uniformity, making them suitable for highly exothermic reactions (Levenspiel, 1999).
- **Radial-Flow Spherical Reactors:** Used in fluidized bed applications, these reactors offer superior gas-solid contact and better heat dissipation. (Rase, 1990)

Each of these configurations presents distinct advantages and limitations in terms of heat management, mass transfer, and reaction kinetics. The choice of reactor geometry is often dictated by process-specific requirements, particularly for reactions involving multiple phases or complex reaction networks.

4.2 *Advancements in Reactor Optimization*

Beyond conventional designs, researchers have focused on optimizing reactor performance through mathematical modelling and novel reactor shapes. One of the key advancements in reactor optimization is the Attainable Region (AR) Theory, which provides a framework for determining optimal reactor configurations using

geometric methods. This approach has been successfully applied to improve conversion efficiency in various catalytic processes (Glasser et al., 1987).

Similarly, Computational Fluid Dynamics (CFD) simulations have been employed to analyze reactor flow dynamics, pressure profiles, and catalyst distribution. Studies have demonstrated that non-conventional reactor geometries can significantly influence the reaction environment by modifying residence time distribution and improving heat management (Moletta, 2005).

4.3 *Frustum Geometry in Reactor Design*

One of the emerging concepts in reactor design is the use of frustum-shaped reactors, where the reactor cross-sectional area changes along its length. This configuration has been proposed as a means to enhance reaction performance without modifying feed conditions or increasing catalyst volume.

Several studies have investigated the benefits of frustum geometries:

- **Pressure Distribution and Reaction Kinetics:** A gradual change in reactor diameter can lead to controlled pressure drop, which is beneficial for maintaining optimal reaction conditions, particularly for gas-phase reactions (Iliuta & Larachi, 2004).
- **Catalyst Utilization:** The variation in reactor cross-section affects catalyst loading and distribution, which in turn influences mass transfer and reaction rates. This has been demonstrated in catalytic cracking and hydroprocessing applications (Rahimpour et al., 2011).
- **Temperature Control:** The frustum shape can help regulate temperature gradients, reducing the risk of hot spots in exothermic reactions, as observed in oxidation and dehydrogenation processes (Doraiswamy & Kulkarni, 2014).

4.4 *Application of Frustum Reactors in Industrial Processes*

Frustum-shaped reactors have been explored in different chemical reactions, including:

- **Liquid-Phase Isomerization of Normal Butane:** This process benefits from improved temperature control and enhanced catalyst distribution, leading to higher selectivity towards isobutane.
- **Gas-Phase Oxidation of Ethylene with Air:** Oxidation reactions require precise control over reactant mixing and residence time, which the frustum geometry can facilitate.

- Gas-Phase Olefin Production via Paraffin Dehydrogenation: Maintaining favorable pressure conditions along the reactor is critical for improving olefin yield, making the frustum design a promising approach.

Recent computational and experimental studies suggest that integrating frustum geometry into reactor design could provide significant improvements in reaction efficiency and product selectivity (Shah et al., 2018). However, further research is needed to validate these findings in large-scale industrial applications.

The evolution of reactor design has been driven by the need to enhance reaction efficiency, optimize energy consumption, and improve catalyst utilization. While conventional reactor geometries have been extensively studied, emerging configurations such as frustum-shaped reactors present promising opportunities for industrial applications. Future work should focus on experimental validation and techno-economic analysis to establish the feasibility of these designs in commercial chemical processes.

5. Methodology

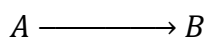
In liquid-phase reactions, the concentration of reactants is insignificantly affected by even relatively large changes in the total pressure. Consequently, we can totally ignore the effect of pressure drop on the rate of reaction when sizing liquid-phase chemical reactors. However, in gas-phase reactions, the concentration of the reacting species is proportional to the total pressure and consequently, proper accounting for the effects of pressure drop on the reaction system can, in many instances, be a key factor in the success or failure of the reactor operation. (Fogler, 2010)

For gas-phase reactions pressure drop may is important to understand because of its effect on concentrations and rate laws. For an ideal gas, the concentration of reacting species i is

$C_i = C_{i0} \left(\frac{\theta + v_i X_i}{1 + \varepsilon X} \right) \frac{P}{P_0} \frac{T_0}{T}$	(1)
--	-----

One must determine the ratio P/P_0 as a function of volume V or the catalyst weight, W , to account for pressure drop. then it can combine the concentration, rate law, and design equation. However, whenever accounting for the effects of pressure drop, the differential form of the mole balance (design equation) must be used.

If, for example(Fogler, 2010), the second-order isomerization reaction.



is being carried out in a packed-bed reactor, the differential form of the mole balance equation in terms of catalyst weight is

$F_{A0} \frac{dX}{dW} = -r'_A$	(2)
--------------------------------	-----

Where:

$-r'_A = kC_A^2$	(3)
------------------	-----

According to ideal gas, the rate becomes

$-r'_A = k \left(C_{A0} \left(\frac{1 + X_A}{1 + \varepsilon X} \right) \frac{P}{P_0} \frac{T_0}{T} \right)^2$	(4)
--	-----

Note from Equation above equation that the larger the pressure drop (i.e., the smaller P) from frictional losses, the smaller the reaction rate! and assuming isothermal operation ($T = T_0$) to understand the pressure effect only

Combining the rate equation with the mole balance

$\frac{dX}{dW} = \frac{kC_{A0}}{v_0} \left(\frac{1 + X_A}{1 + \varepsilon X} \right)^2 \left(\frac{P}{P_0} \right)^2$	(5)
---	-----

For isothermal operation ($T = T_0$) the right-hand side is a function of only conversion and pressure:

$\frac{dX}{dW} = f(X_A, P)$	(6)
-----------------------------	-----

So, the pressure drop need to relate to the catalyst weight in order to determine the conversion as a function of catalyst weight. The equation used most to calculate pressure drop in a packed porous bed is the Ergun equation.

$\frac{dp}{dz} = - \frac{G}{\rho_0 g_c D_p} \left(\frac{1 - \phi}{\phi^3} \right) \left[\frac{150(1 - \phi)}{D_p} + 1.75G \right] \frac{P_0}{P} \left(\frac{T}{T_0} \right) \frac{F_T}{F_{T0}}$	(7)
--	-----

Where:

$$P = \text{pressure}, \frac{\text{lb}}{\text{ft}^2} \text{ or } \frac{\text{kg}}{\text{m} \cdot \text{h}^2}$$

$$\phi = \text{porosity} = \frac{\text{volume of void}}{\text{total bed volume}}$$

$$1 - \phi = \frac{\text{volume of solid}}{\text{total bed volume}}$$

$$g_c = \left(32.174 \frac{\text{lb.ft}}{\text{s}^2.\text{lb}_f} \right) \text{ or } \left(4.17 \times 10^8 \frac{\text{lb.ft}}{\text{h}^2.\text{lb}_f} \right) (\text{conversion factor})$$

$$(\text{recall that for the metric system } g_c = 1.0)$$

$$D_p = \text{diameter of particle in the bed, ft or m}$$

$$\mu = \text{viscosity of gas passing through the bed, } \frac{\text{lb}_m}{\text{ft.h}} \text{ or } \frac{\text{kg}}{\text{m.h}}$$

$$z = \text{length down the packed bed of pipe, ft or m}$$

$$\rho_0 = \text{gas density(at initial condition), } \frac{\text{lb}}{\text{ft}^3} \text{ or } \frac{\text{kg}}{\text{m}^3}$$

$$G = \rho u = \text{superficial mass velocity, } \left(\frac{\text{g}}{\text{cm}^2.\text{s}} \right) \text{ or } \left(\frac{\text{lb}}{\text{ft}^2.\text{h}} \right)$$

$$u = \text{superficial velocity} = \frac{\text{volumetric flow}}{\text{cross sectional area of pipe}}, \frac{\text{ft}}{\text{h}} \text{ or } \frac{\text{m}}{\text{h}}$$

$$G = \frac{\dot{m}}{A_c}$$

$$\dot{m} = \text{mass flow rate, } \frac{\text{lb}}{\text{h}} \text{ or } \frac{\text{kg}}{\text{h}}$$

$$A_c = \text{cross sectional area of pipe, ft}^2 \text{ or m}^2$$

$$\frac{F_T}{F_{T0}} = (1 + \varepsilon X_A)$$

$$\varepsilon = y_{A0} \cdot \delta$$

as the rate equation based in the catalyst weight and usually in the tubular packed-bed reactors we are more interested in catalyst weight rather than the distance z down the reactor. The catalyst weight up to a distance of z down the reactor is,

$W = (1 - \phi) \cdot A_c \cdot z \cdot \rho_c$	(8)
$\left[\begin{matrix} \text{weight of} \\ \text{catalyst} \end{matrix} \right] = \left[\begin{matrix} \text{volume of} \\ \text{solids} \end{matrix} \right] \times \left[\begin{matrix} \text{density of} \\ \text{solid catalyst} \end{matrix} \right]$	(9)
$\frac{dW}{dz} = \rho_c (1 - \phi) \pi [r_i^2 + 2r_i z m + z^2 m^2] \rightarrow \text{frustum}$	(10)
$\frac{dW}{dz} = \rho_c (1 - \phi) \pi r^2 \rightarrow \text{tube}$	(11)

r_i = inlet redus for the frustum geometry

z = the axial distance

m = the slop of the frustum

$(1 - \phi) \cdot \rho_c = \rho_B$ bluk density

These two equations can be used to change the Ergon equation from distance depended to catalyst weight depended by substitute dz with its value based in frustum or tube geometry.

We collect the differential equations together

$\frac{dX}{dW} = \frac{kC_{A0}}{v_0} \left(\frac{1 + X_A}{1 + \varepsilon X} \right)^2 \left(\frac{P}{P_0} \right)^2$	(12)
$\frac{dP}{dW} = \frac{-\frac{G}{\rho_0 g_c D_p} \left(\frac{1 - \phi}{\phi^3} \right) \left[\frac{150(1 - \phi)}{D_p} + 1.75G \right] \frac{P_0}{P} \left(\frac{T}{T_0} \right) \frac{F_T}{F_{T0}}}{\rho_c(1 - \phi)\pi[r_i^2 + 2r_i z m + z^2 m^2]}$	(13)

Or other couple can create depend in the rate type

$\frac{dX}{dz} = \frac{kC_{A0}}{v_0} \rho_c(1 - \phi)\pi[r_i^2 + 2r_i z m + z^2 m^2] \left(\frac{1 + X_A}{1 + \varepsilon X} \right)^2 \left(\frac{P}{P_0} \right)^2$	(14)
$\frac{dp}{dz} = -\frac{G}{\rho_0 g_c D_p} \left(\frac{1 - \phi}{\phi^3} \right) \left[\frac{150(1 - \phi)}{D_p} + 1.75G \right] \frac{P_0}{P} \left(\frac{T}{T_0} \right) \frac{F_T}{F_{T0}}$	(15)

Here it's clear that we have reached two coupled first-order differential equations, that must be solved simultaneously. A variety of software packages and numerical integration schemes are available for this purpose.

More notes can be identified here that when $m = \text{zero}$ the differential equation will explain the tube geometry other wase will give frustum geometry

$\frac{dX}{dW} = f_1(X_A, P)$	(16)
$\frac{dP}{dW} = f_2(X_A, P)$	(17)

In this study, we aim to analyze the applicability of frustum reactor geometry in industrially relevant reactions rather than purely academic scenarios. Specifically, we will examine a liquid-phase reaction, the isomerization of normal butane, considering that liquid-phase reactions are generally unaffected by pressure variations. This aspect aligns with the theoretical foundation of the frustum reactor;

however, our focus will be on studying reaction rate variations and their control parameters. Additionally, we will investigate two gas-phase reactions: ethylene oxide production via vapor-phase catalytic oxidation of ethylene with air (negative epsilon reaction) and olefin production via paraffin dehydrogenation in a reformer (positive epsilon reaction). The outcomes of these reactions will provide insight into both the advantages and limitations of implementing frustum geometry in catalytic processes.

In all three reactions, the simulation compares the performance of cylindrical and frustum geometries reactors of equal volume.



$$V = \pi r^2 z$$

$$\frac{dV}{dz} = \pi r^2$$

$$dV = \pi r^2 dz$$

Substitute in the design equation for
tubular reactor

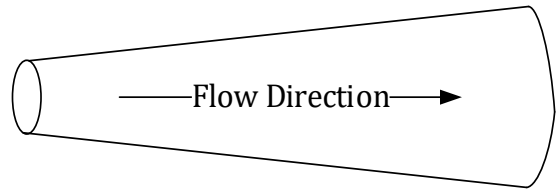
⇒ Transient plug flow reactor

$$-\frac{\partial F_A}{\partial V} + r_A = \frac{\partial C_A}{\partial t}$$

$$-\frac{F_{A0}}{\pi r^2} \frac{\partial x_A}{\partial z} + r_A = C_{A0} \frac{\partial x_A}{\partial t}$$

⇒ Steady state plug flow reactor

$$\frac{\partial F_A}{\partial V} = r_A$$



$$V = \frac{\pi z}{3} (3r_i^2 + 3r_i m z + (m z)^2)$$

$$V = \pi z r_i^2 + \pi r_i m z^2 + \frac{\pi m^2 z^3}{3}$$

$$\frac{dV}{dz} = \pi r_i^2 + 2\pi r_i m z + \pi m^2 z^2$$

$$dV = (\pi r_i^2 + 2\pi r_i m z + \pi m^2 z^2) dz$$

Substitute in the design equation for
tubular reactor

⇒ Transient plug flow reactor

$$-\frac{\partial F_A}{\partial V} + r_A = \frac{\partial C_A}{\partial t}$$

$$\frac{-F_{A0}}{(\pi r_i^2 + 2\pi r_i m z + \pi m^2 z^2)} \frac{\partial x_A}{\partial z} + r_A = C_{A0} \frac{\partial x_A}{\partial t}$$

⇒ Steady state plug flow reactor

$$\frac{\partial F_A}{\partial V} = r_A$$

$$\frac{F_{A0}}{\pi r^2} \frac{\partial x_A}{\partial z} = r_A \quad \left| \quad \frac{F_{A0}}{(\pi r_i^2 + 2\pi r_i m z + \pi m^2 z^2)} \frac{\partial x_A}{\partial z} = r_A \right.$$

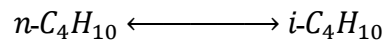
5.1 Liquid-Phase Isomerization of Normal Butane (Fogler, 2016)

Normal butane, C_4H_{10} is to be isomerized to isobutane in a plug-flow reactor. Isobutane is a valuable product that is used in the manufacture of gasoline additives. For example, isobutane can be further reacted to form isooctane. The 1996 selling price of n-butane was 37.2 cents per gallon, while the price of isobutane was 48.5 cents per gallon.

The reaction is to be carried out adiabatically in the liquid phase under high pressure using essentially trace amounts of a liquid catalyst which gives a specific reaction rate of 3.11 h^{-1} at 360 K. Calculate the PFR velum necessary to process 100,000 gal/day (163 kg mol/h) of a mixture 90 mol % n-butane and 10 mol % i-pentane, which is considered an inert. The feed enters at 330 K.

The result from the example gives the conversion of 0.7 at a volume of 2.6 m³. During this study it's more important to understand the conversion as a function in the length of the reactor to know if the geometry make any different. The maximum length will be 6 m in the three cases and the radius will be modify to give volume of 2.6 m³.

The following is the kinetic and reaction data



$$C_{A0} = 9.3 \frac{\text{kgmol}}{\text{m}^3}$$


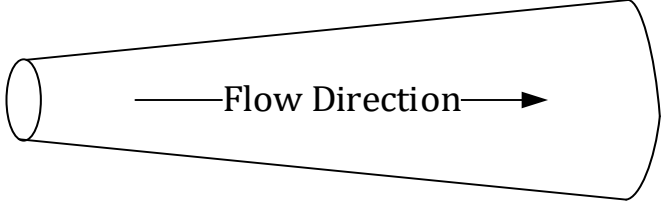
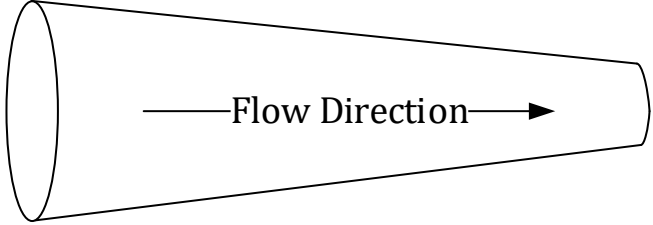
$$F_{A0} = 146.7 \frac{\text{kgmol}}{\text{hr}}$$

$$k = 31.1 \exp\left(\frac{65,700}{8.314} \left(\frac{1}{360} - \frac{1}{330 + 43.3 * x_A}\right)\right) \rightarrow (\text{hr}^{-1})$$

$$K_C = 3.03 \exp\left(\frac{-6,900}{8.314} \left(\frac{1}{333} - \frac{1}{330 + 43.3 * x_A}\right)\right)$$

$$-r_A = k C_{A0} \left[1 - \left(1 + \frac{1}{K_C}\right) x_A\right] \rightarrow \left(\frac{\text{kgmol}}{\text{hr} * \text{m}^3}\right)$$

The shapes that are used in this study and their dimension

Tube		$r = 0.37 \text{ m}$ $z = 6 \text{ m}$ $Volume = 2.6 \text{ m}^3$
Positive Frustum		$r_i = 0.15 \text{ m}$ $r_o = 0.555 \text{ m}$ $m = 0.0675$ $z = 6 \text{ m}$ $Volume = 2.6 \text{ m}^3$
Negative Frustum		$r_i = 0.555 \text{ m}$ $r_o = 0.15 \text{ m}$ $m = -0.0675$ $z = 6 \text{ m}$ $Volume = 2.6 \text{ m}^3$

Q-Basic program is used to solve for conversion as a function of z after each period of time. 110 iterations of $\Delta t = \Delta z = 0.1$ are used. Tube as well as + and – frustums have been investigated as transients and at steady state.

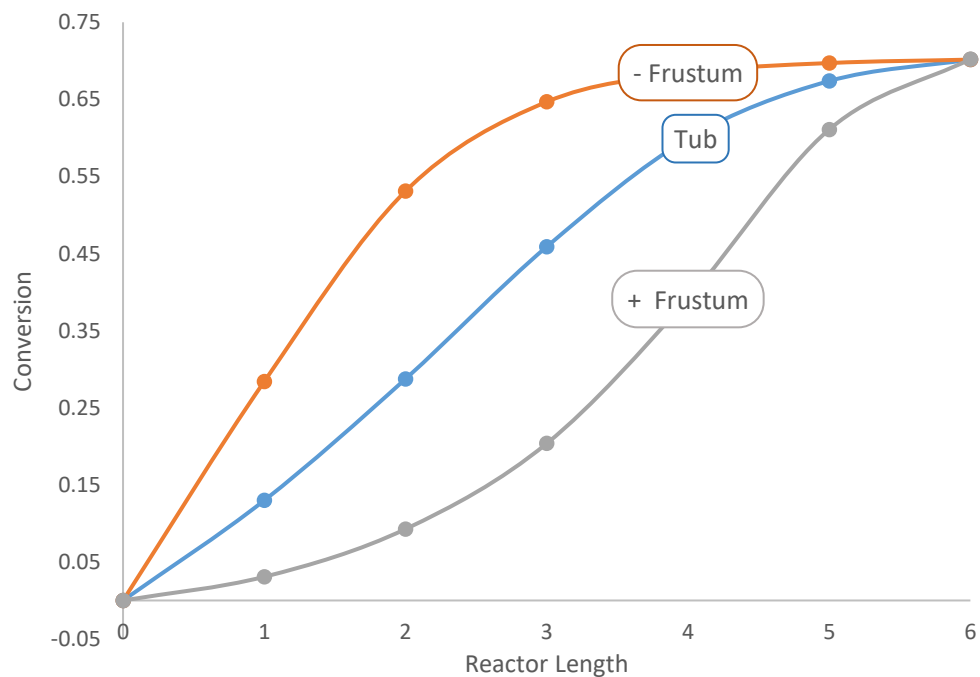
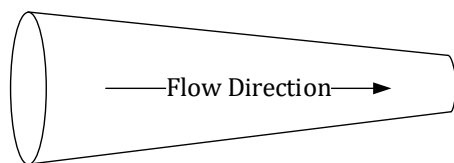


Figure 2 Steady state curves for all geometry



$(r_i = 0.555 \text{ m}) \text{ \& } (m = -0.0675) \text{ \& } (z = 6)$

total volume = 2.6 m^3

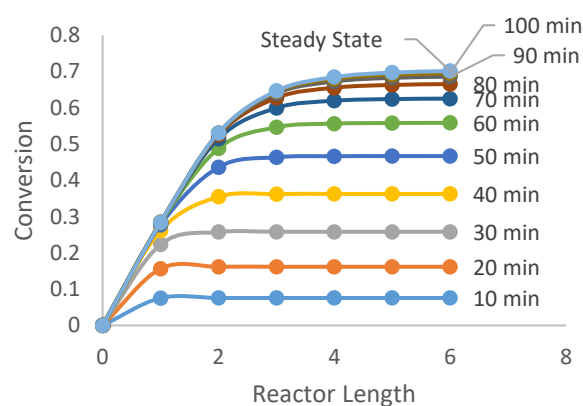


Figure 3 Unsteady state for – frustum

Table 1 Show the steady state result

z	X
0	0
1	0.2840487
2	0.5308967
3	0.64679465
4	0.6846393
5	0.6971129
6	0.701552



$(r = 0.37 \text{ m}) \text{ \& } (z = 6 \text{ m})$

total volume = 2.6 m^3

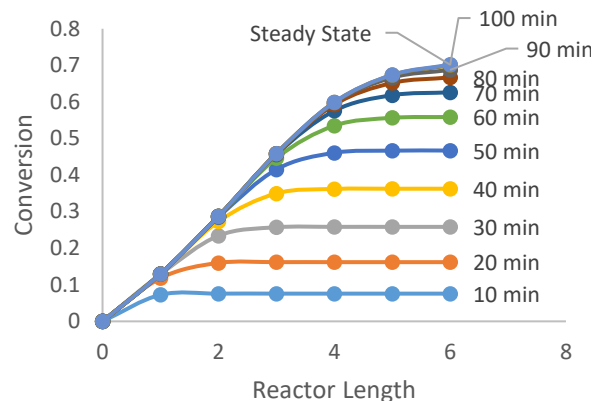
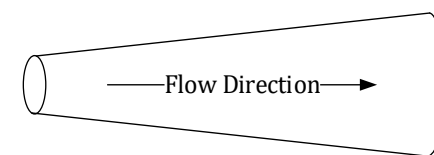


Figure 4 Unsteady state for normal tube

Table 2 Show the steady state result

Z	x
0	0
1	0.1298191
2	0.2873462
3	0.4588511
4	0.5990537
5	0.67379
6	0.7017201



$(r_i = 0.15 \text{ m}) \text{ \& } (m = 0.0675) \text{ \& } (z = 6)$

total volume = 2.6 m^3

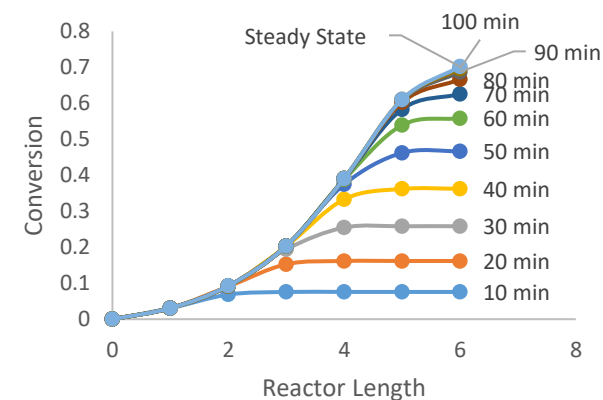


Figure 5 Unsteady state for + frustum

Table 3 show the steady state result

Z	x
0	0
1	0.030718
2	9.26E-02
3	0.2036166
4	0.3910332
5	0.610921
6	0.7021851

Comparing + and – frustum to normal tubes, the result prove that the geometry has a direct effect on conversion so it's starts to be important to know the direct relation between the slope of the part of frustum and the conversions. Taking more geometry for the study start from part of frustum with slope of -0.1 to slope 0.1 that will give more ideas to understand the behavior of the geometry effect.

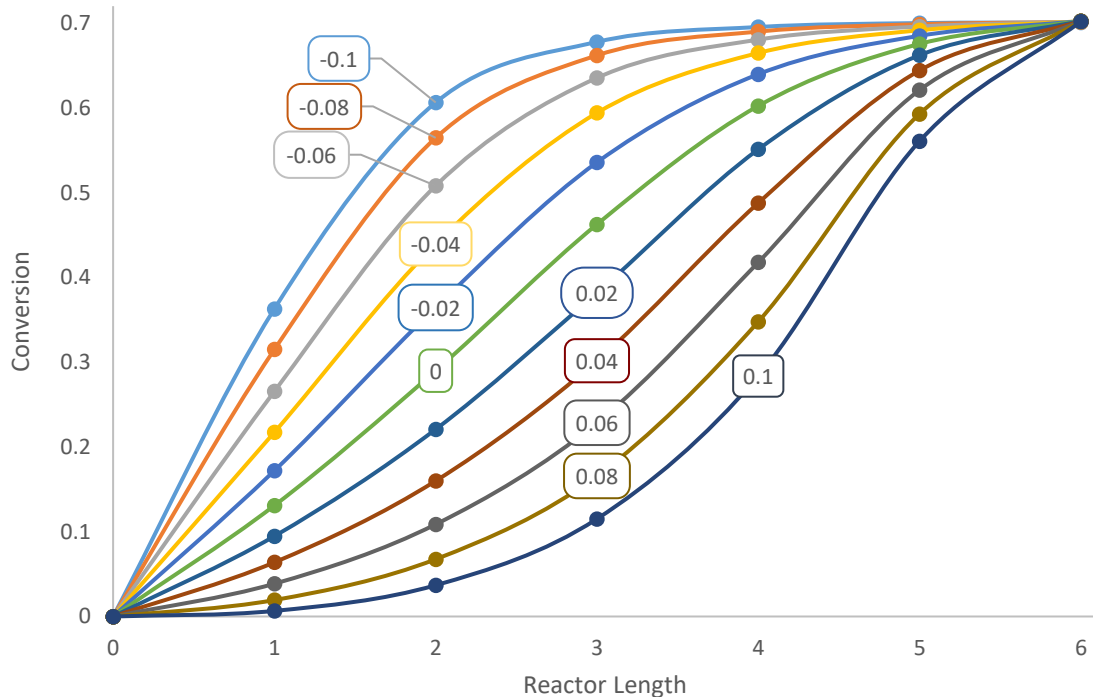


Figure 6 Show the steady state conversion at different part of frustum geometry

It's clear that the negative part of frustum gives a good result more than the tube or the positive part of frustum. In the case $m = 0.0675$ the conversion of 0.65 is achieved at 3 m, so this mean a small negative part of with a volume of 1.97 m³ reach 0.65 \approx 0.7 conversion where a volume of 2.6 m³ is necessary in the tube geometry to reach 0.7 conversion for the butane isomerization.

The rate behavior of the different cases.

$$-r_A = \overbrace{kC_{A0}}^A \left[\overbrace{1 - \left(1 + \frac{1}{K_C}\right)x_A}^B \right]$$

The rate equation will be divided into two part (A & B) the understand of increasing and decreasing of these two parts will explain the behavior of rate equation. Where part A represent the rate of isomerization and B represent the equilibrium of the isomerization however it can be clear from the following table where the beak of the rate will be in the reactor.

If the beak position change from each reactor it may be clear that even in liquid reaction the frustum can give a new behavior that can be interested and use from a control engineer.

Table 4 show the result of the tube geometry

A	B	z	r_A
39.31804	1	0	39.31804
58.77183	0.82649	1	48.57432978
94.03589	0.6110534	2	57.46095031
153.6247	0.3703249	3	56.89105167
255.9957	0.1686999	4	43.18644899
276.1476	5.94E-02	5	16.41213948
297.3499	1.83E-02	6	5.434684937

Table 5 show the result of the positive part of frustum

A	B	z	r_A
39.31804	1	0	39.31804
43.29487	0.9592708	1	41.53150458
52.36053	0.8773258	2	45.93724387
73.42127	0.7262353	3	53.32111804
126.8417	0.46629	4	59.14501629
233.3604	0.1514327	5	35.33839545
297.7151	1.76E-02	6	5.236912809

Table 6 show the result of the negative part of frustum

A	B	z	r_A
39.31804	1	0	39.31804
93.13314	0.615619	1	57.33449
187.6408	0.267262	2	50.14924
256.9705	9.90E-02	3	25.45159
284.2145	4.35E-02	4	12.35384
293.7536	2.51E-02	5	7.366726
297.218	1.85E-02	6	5.506044

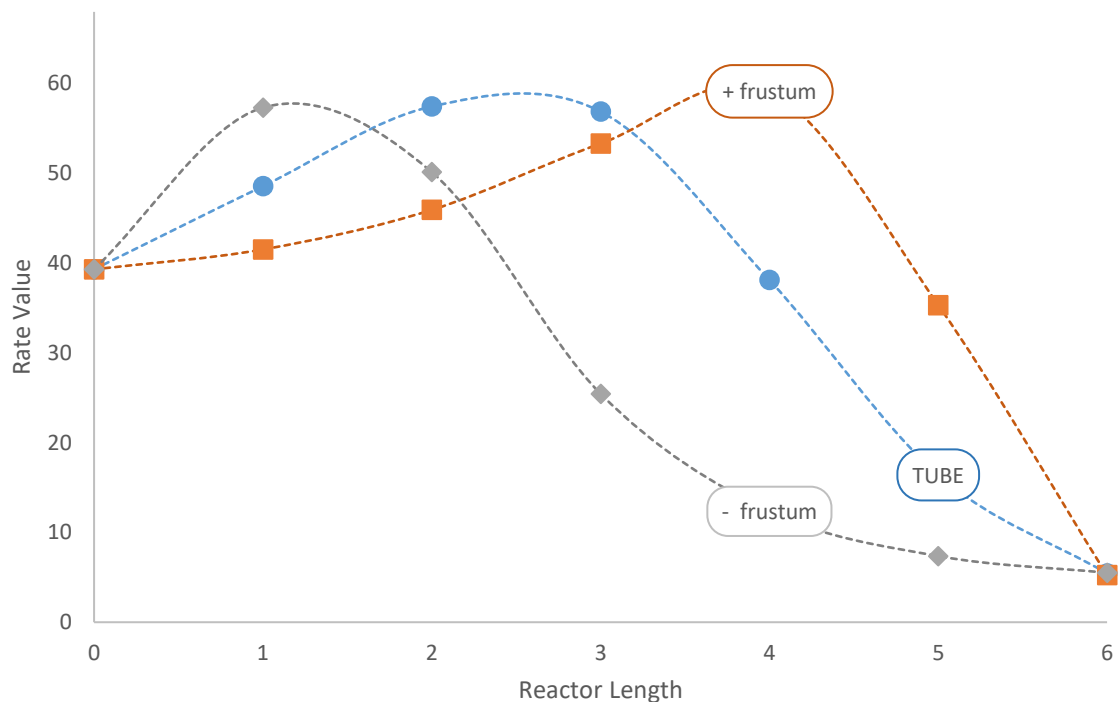


Figure 7 Show the rate behavior at the three geometries of the PFR

Table 7 show the summary of the simulation results

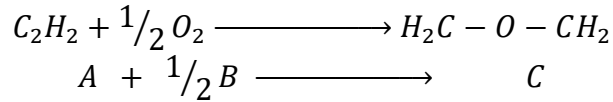
Geometry	Final conversion	The position of the rate peak (m)	The position of - 10% of the final conversion (m)	Study state time (min)
Tube	0.7017201	2.4	4.434	100
+ Frustum	0.7021851	4	4.434	100
- Frustum	0.701552	1	4.434	100

"The positive frustum's final conversion may achieve slightly better results compared to the tube for this reaction; however, the improvement remains insignificant."

5.2 Ethylene oxide by vapor-phase catalytic oxidation of ethylene with air (Negative epsilon). (Fogler, 2016)

Approximately 7 billion pounds of ethylene oxide were produced in the United States in 1997. The 1997 selling price was \$0.58 a pound, amounting to a commercial value of \$4.0 billion. Over 60% of the ethylene oxide produced is used to make ethylene glycol. The major end uses of ethylene oxide are antifreeze (30%), polyester (30%), surfactants (10%), and solvents (5%). (H Scott, 2006)

We want to calculate the conversion of each reactor with 27.8 kg of catalyst weight necessary when ethylene oxide is to be made by the vapor-phase catalytic oxidation of ethylene with air.



Ethylene and oxygen are fed in stoichiometric proportions to a packed-bed reactor operated isothermally at 260°C. Ethylene is fed at a rate of 0.13607 *kg mol/s* at a pressure of 1013.25 kPa. It is proposed to use 10 banks of 0.4572 *m* in diameter schedule 40 tubes packed with catalyst with 100 tubes per bank. Consequently, the molar flow rate to each tube is to be 489.88 *g mol/hr*. The properties of the reacting fluid are to be considered identical to those of air at this temperature and pressure. The density of the 6.35x10⁻³ *m* catalyst particles is 1920 *kg/m³* and the bed void fraction is 0.45. The rate law is

$$\begin{aligned} -r'_A &= k P_A^{1/3} P_B^{2/3} \quad \frac{lb \text{ mol}}{lb \text{ cat. hr}} \\ k &= 0.0141 \text{ lb} \quad \frac{lb \text{ mol}}{atm. lb \text{ cat. hr}} @ 260^\circ C \end{aligned}$$

The design equation for the tubular reactor

$$\frac{dx_A}{dw} = \frac{-r_A}{F_{A0}} \quad (18)$$

The rate equation will have the following formula

$$-r_A = k \left(\frac{1}{2} \right)^{2/3} \left(\frac{P P_{A0}}{P_0} \right) \left(\frac{1 - x_A}{1 + \varepsilon x_A} \right) \quad (19)$$

The pressure drop will be calculated using Ergun equation which will have the following formula in this application

$$\frac{dP}{dz} = - \frac{\dot{m}(1 - \phi)}{A_c \rho_0 D_p \phi^3} \left(\frac{150 (1 - \phi) \mu}{D_p} - \frac{1.75 \dot{m}}{A_c} \right) \left(\frac{P_0}{P} \right) (1 + \varepsilon x_A) \quad (20)$$

The catalyst distribution along the reactor


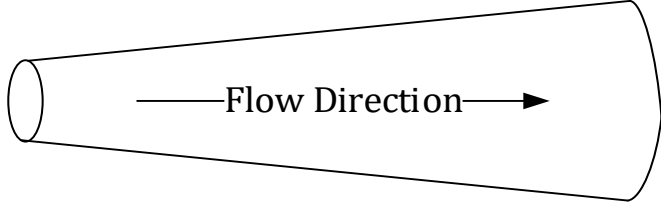
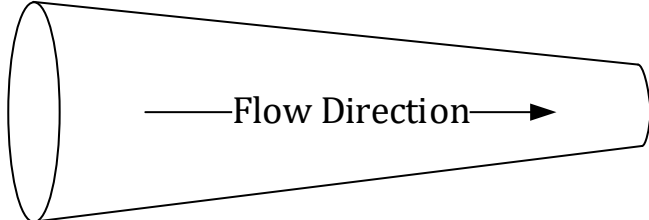
$$\frac{dw}{dz} = \rho_c (1 - \phi) \pi (r_i^2 + 2 z r_i m + z^2 m^2) \quad (21)$$

$$w = \rho_c (1 - \phi) \left(\frac{\pi z}{3} (3r_i^2 + 3 z r_i m + z^2 m^2) \right) \quad (22)$$

The numerical value for all parameters are shown below:

Entrance condition	Kinetic data	Catalyst property
$\dot{m} = 47.355 \frac{kg}{hr}$	$k = 0.1392 \frac{gmol}{Kpa. kgcat. hr}$	$\rho_c = 1922.22 \frac{kg}{m^3}$
$F_{A0} = 489.88 \frac{gmol}{hr}$	$\varepsilon = -0.15$	$D_p = 0.00635 \text{ m}$
$\rho_0 = 6.6156 \frac{kg}{m^3}$		$\phi = 0.45$
$\mu = 0.1002 \frac{kg}{m \text{ hr}}$		$w = 27.8 \text{ kg}$
$P_{A0} = 303.975 \text{ Kpa}$		
$P_0 = 1013.25 \text{ Kpa}$		

Based on catalyst weight of 27.8 kg the volume and the dimension of the three reactors will be

Tube		$r = 0.02045 \text{ m}$ $z = 20 \text{ m}$ $Volume = 0.0263 \text{ m}^3$
Positive Frustum		$r_i = 0.01842 \text{ m}$ $r_o = 0.02242 \text{ m}$ $m = 0.0002$ $z = 20 \text{ m}$ $Volume = 0.0263 \text{ m}^3$
Negative Frustum		$r_i = 0.02242 \text{ m}$ $r_o = 0.01842 \text{ m}$ $m = -0.0002$ $z = 20 \text{ m}$ $Volume = 0.0263 \text{ m}^3$

The previous differential equations can be coupled to yield the following equations which are solved together by the polymath.

$$\frac{dx_A}{dz} = k \left(\frac{1}{2} \right)^{2/3} \left(\frac{P P_{A0}}{F_{A0} P_0} \right) \left(\frac{1 - x_A}{1 + \varepsilon x_A} \right) \rho_c (1 - \phi) \pi (r_i^2 + 2 z r_i m + z^2 m^2) \quad (23)$$

$$\frac{dP}{dz} = - \frac{\dot{m}(1 - \phi)}{A_c \rho_0 D_p \phi^3} \left(\frac{150 (1 - \phi) \mu}{D_p} - \frac{1.75 \dot{m}}{A_c} \right) \left(\frac{P_0}{P} \right) (1 + \varepsilon x_A) \quad (24)$$

The above equations describe the behavior of conversion and the pressure distribution as in fig 8 and 9 with reactor length. The slope value (m) is the geometry parameter: if it's value zero all the differential will be describing the tube geometry, the positive and negative value will explain the two positions of the frustum. It's clear that the geometry changes conversion behavior, the negative frustum gives a high conversion compared to other geometries. System pressure is lower than other geometries along the length of the reactor. The results for tube as well as +and - frustums are shown in figure below.

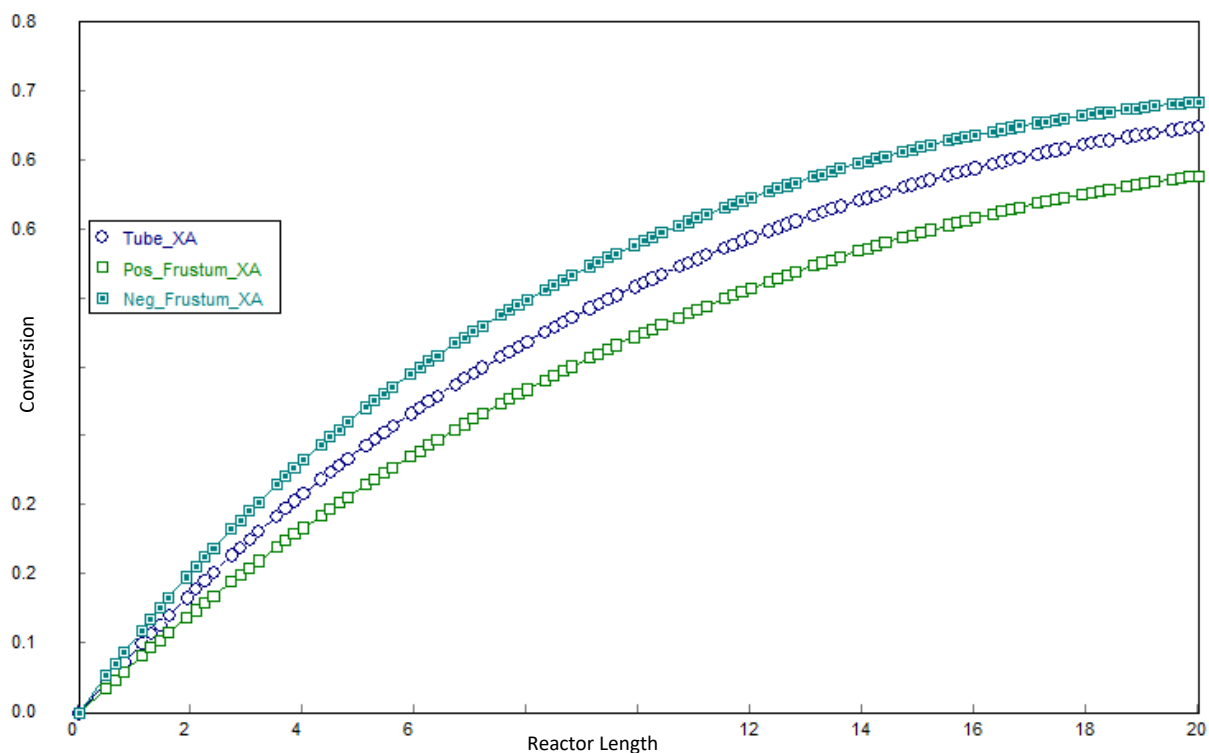


Figure 8 show the behavior of the conversion with the reactor length

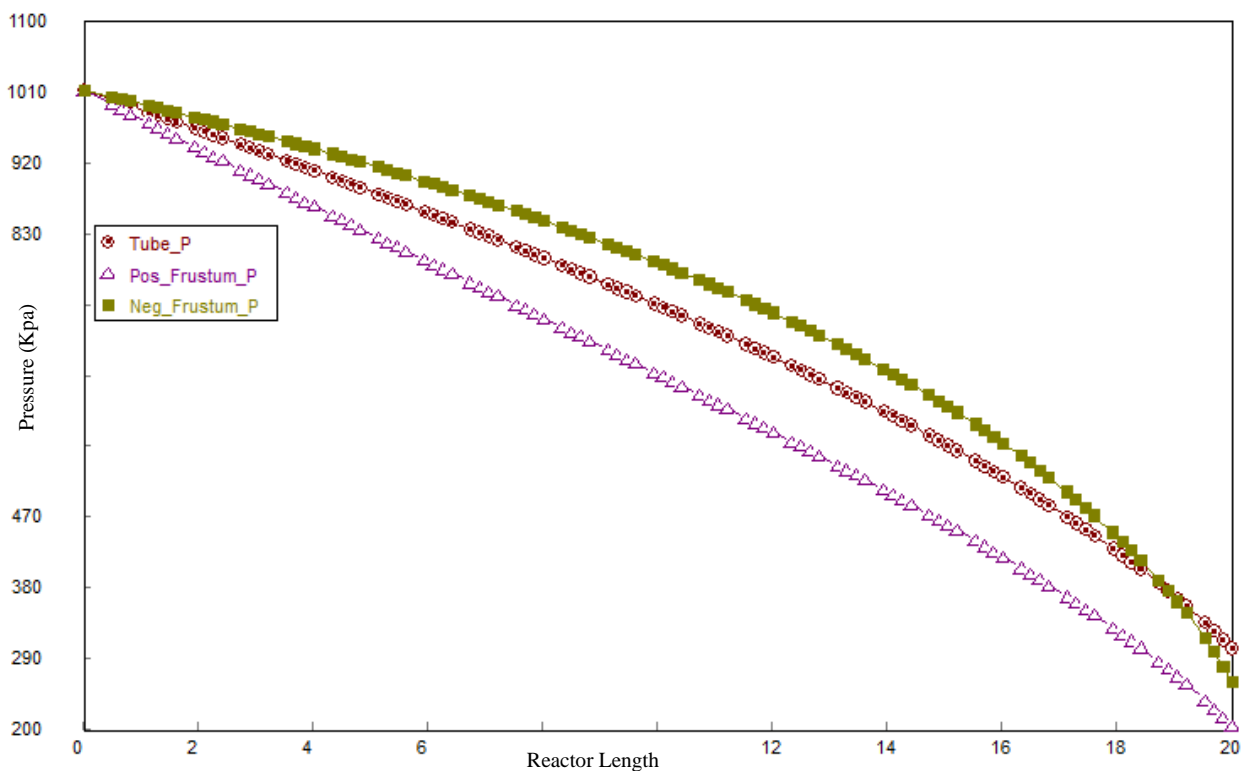


Figure 9 show the pressure distribution along the reactor length

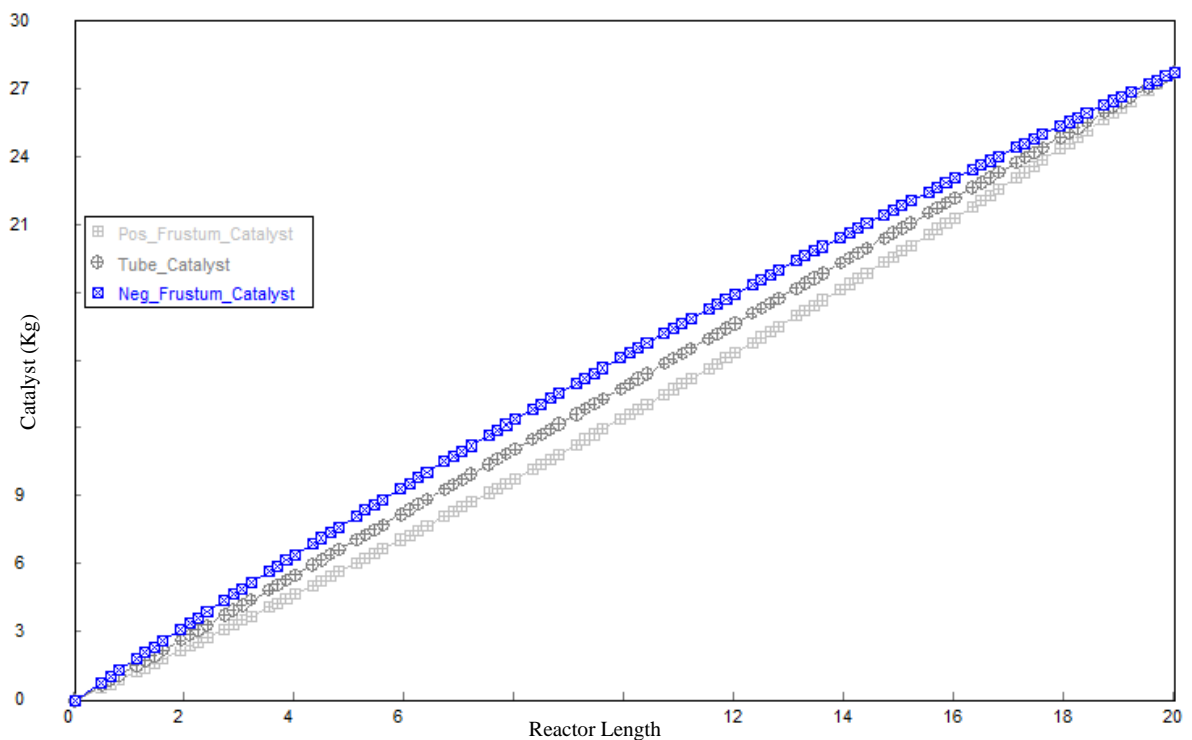


Figure 10 The catalyst weight based in the reactor length

Table 8 the average θ slope change of the pressure drops in the reactors

The geometry	First two meters	Medium Two Meter	Final two meters
Tube	-87.7156	-88.1756	-89.0698
Positive Frustum	-88.4543	-88.4115	-89.0607
Negative Frustum	-86.7829	-88.0466	-89.3793

Depending on geometry reactors with the same amount of catalyst have different conversion and pressure drops. It can be noted that the Negative frustum geometry minimizes pressure drop except in the last 2 meters where a high pressure drop occurs, this may be due to large number of fine catalyst particles that fills that area thus enabling the Negative frustum a higher 3% conversion.

Table 9 show the final result of pressure & conversion

Geometry	Finial Conversion	Final Pressure (kPa)
Tube	0.6792	305.1
Positive Frustum	0.6221	205.8
Negative Frustum	0.7076	262.5

Table 10 a sensitive analysis for the first & last two meter in the reactors

Geometry	Pressure drops in first 2 meter	Conversion increase in first 2 meter	Pressure drops in last 2 meter	Conversion increase in last 2 meter
Tube	52.3	0.143	126.6	0.021
Positive Frustum	77.4	0.119	125.5	0.022
Negative Frustum	37.08	0.168	198.4	0.016

When the flow rate in one tube is 47.355 kg/hr , for 1000 units the saving in amount of catalyst:

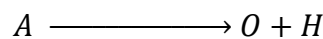
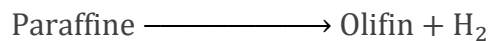
$$\text{using - frustum over tube} = 47.355 * (0.7076 - 0.6792) * 1000 = 1344.88 \frac{\text{kg}}{\text{hr}}$$

$$\text{using tube over + frustum} = 47.355 * (0.6792 - 0.6221) * 1000 = 2703.97 \frac{\text{kg}}{\text{hr}}$$

It's clear now that negative the frustum with small slope of -0.0002 is better than tubes, even though in the final two meters the pressure drop increases suddenly due to the small diameter and catalyst size that decreases void fraction which in turn affects pressure

5.3 Olefin by paraffin Dehydrogenation Reaction in reformer (Positive epsilon). (Fogler, 2016)

Reforming reactors are used to increase the octane amount of petroleum. In a reforming process, 20,000 barrels of petroleum are to be processed per day. The corresponding mass and molar feed rates are 44 kg/s and 440 mol/s, respectively. In the reformer, dehydrogenation reactions such as



occur. The reaction is first order in paraffin. Assume that pure paraffin enters the reactor at a pressure of 2000 kPa and a corresponding concentration of 0.32 mol/dm³. Calculate the pressure drops and conversion when the reaction is carried out in a tubular packed bed, positive frustum and negative frustum. The catalyst weight is the same in each reactor, 173,870 kg.

the rate equation is

$$-r'_A = k' C_A$$

$$-r_A = \rho_B (-r'_A) = \rho_C (1 - \Phi) (-r'_A) = \rho_C (1 - \Phi) (k' C_A)$$

$$y = \frac{P}{P_0}$$

The design equation for the tubular reactor

$$\frac{dx_A}{dw} = \frac{-r_A}{F_{A0}} \quad (25)$$

The rate equation will have the following formula

$$-r_A = k' \rho_C (1 - \Phi) C_{A0} \left(\frac{1 - x_A}{1 + \epsilon x_A} \right) y \quad (26)$$

The pressure drop will be calculated using Ergun equation which will have the following formula in this application

$$\frac{dy}{dz} = - \frac{\dot{m}(1 - \Phi)}{A_C \rho_0 D_P \Phi^3} \left(\frac{150 (1 - \Phi) \mu}{D_P} - \frac{1.75 \dot{m}}{A_C} \right) \left(\frac{1 + \epsilon x_A}{y P_0} \right) \quad (27)$$

The catalyst distribution along the reactor


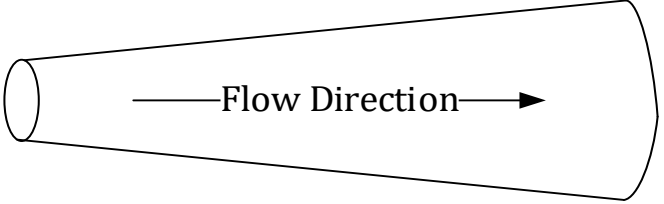
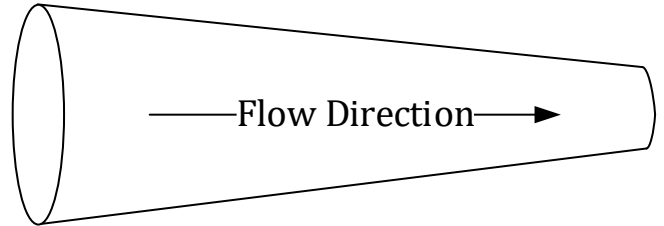
$$\frac{dw}{dz} = \rho_c (1 - \Phi) \pi (r_i^2 + 2 z r_i m + z^2 m^2) \quad (28)$$

$$w = \rho_c (1 - \Phi) \left(\frac{\pi z}{3} (3r_i^2 + 3 z r_i m + z^2 m^2) \right) \quad (29)$$

The numerical value for all parameters is

For kinetic data		For Ergun Pressure drop data	
ρ_c	$2600 \frac{\text{kg}}{\text{m}^3}$	P_0	2000 kPa
Φ	0.4	\dot{m}	$158400 \frac{\text{kg}}{\text{hr}}$
k'	$2e-5$	ρ_0	$32 \frac{\text{kg}}{\text{m}^3}$
C_{A0}	$320 \frac{\text{mol}}{\text{m}^3}$	D_p	0.002
F_{A0}	$440 \frac{\text{mol}}{\text{s}}$	μ	$0.054 \frac{\text{kg}}{\text{m} \cdot \text{hr}}$
ϵ	1		

The dimensions of the three reactors are

Tube		$r = 1.3416 \text{ m}$ $z = 20 \text{ m}$ $\text{Volume} = 113.09 \text{ m}^3$
Positive Frustum		$r_i = 1.1367 \text{ m}$ $r_o = 1.5367 \text{ m}$ $m = 0.02$ $z = 20 \text{ m}$ $\text{Volume} = 113.09 \text{ m}^3$
Negative Frustum		$r_i = 1.5367 \text{ m}$ $r_o = 1.1367 \text{ m}$ $m = -0.02$ $z = 20 \text{ m}$ $\text{Volume} = 113.09 \text{ m}^3$

The previous differential equations can be coupled to yield the following equations which are solved together by the polymath.

Table 11 Show the final result for both conversion and pressure

Geometry	Finial Conversion	Final Pressure (kPa)
Tube	0.778	1413.8
Positive Frustum	0.764	1408.8
Negative Frustum	0.785	1295.4

It's expected to have a high conversion in the large diameter because the components start to have more time in the reactor and for sure that will improve the conversion

In fact, it's the parameter that the frustum plays with it, however if you try to imagine the geometry of the frustum reactor you will note that in a negative frustum the geometry applying a large reactor volume in the beginning which mean large amount of catalysts with a slow time for the component to pass the catalyst even with all of that the pressure drop still play a very important role here.

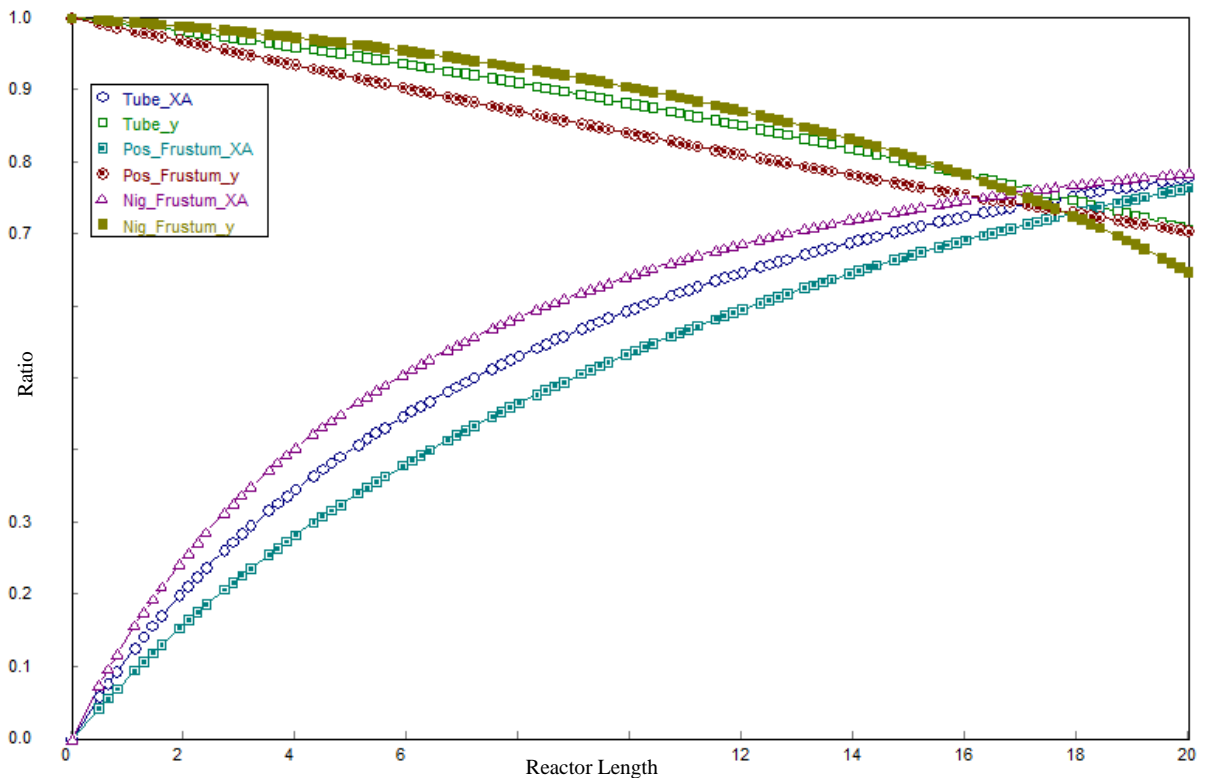


Figure 11 the tube, positive & negative frustum conversion and pressure drop with the new dimensions

Another term that can explain the time of the component remain in the reactor is the superficial velocity fig.13 which is the mass flow rate divided by a cross-sectional area. It is the hypothetical flow velocity which considers that only one type of fluid flows through a given cross-sectional area of the reactor. Hypothetical means that the Superficial Velocity is not the actual velocity in case of multiphase flow. However, in one phase flow the Superficial Velocity is equal to the mean velocity, however it's clear from Ergun equation that by decreasing superficial velocity, the pressure drop will be reduced significantly, resulting in higher conversions.

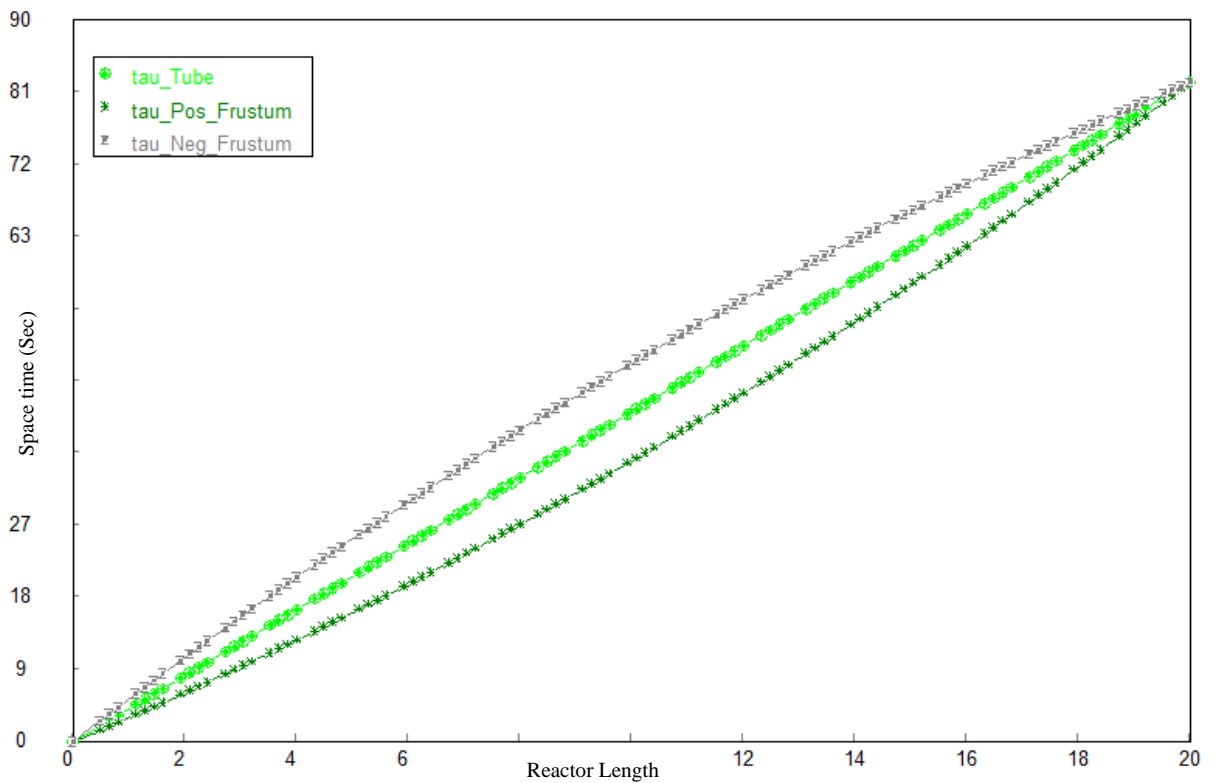


Figure 12 explain the space time (second) for the three reactors

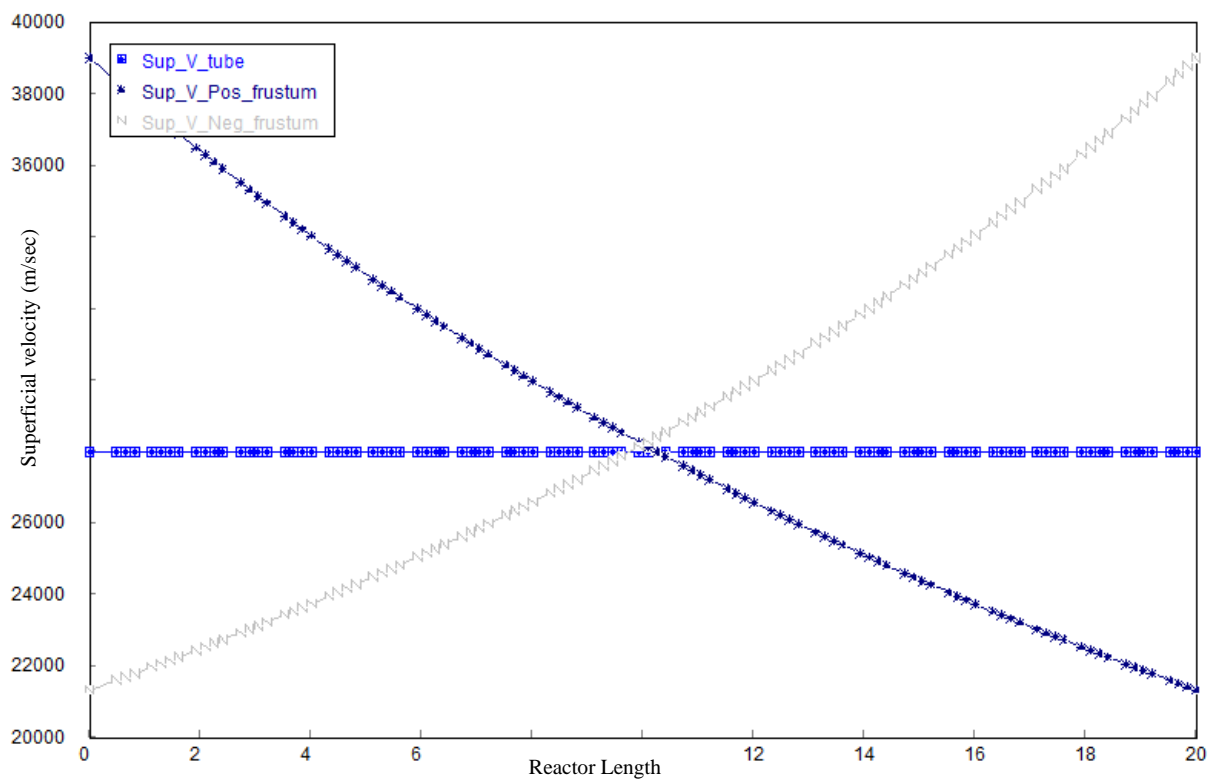


Figure 13 explain the superficial velocity of the three reactors

The above results give a hint about how the geometry can change a lot of parameters which effects the conversion without a change in feed condition.

Table 12 show the summary of the simulation results

20-meter Reactor		
Geometry	Finial Conversion	Final Pressure (kPa)
Tube	0.778	1413.8
+ Frustum	0.764	1408.8
- Frustum	0.785	1295.4

6. Summary of Analysis of Frustum Geometry in Gas and Liquid Phase Reactions

The study focuses on the critical role of pressure in gas-phase reactions and evaluates the performance of frustum geometry compared to standard tube designs. Three distinct gas-phase reactions were analyzed:

- Olefin by Paraffin Dehydrogenation, representing reactions with an increasing number of moles.
- Oxidation of Ethylene with Air, representing reactions with a decreasing number of moles.

Each reaction was examined under standard tube reactor conditions and using a frustum reactor where the effects of altering the inlet direction—from small to large diameter and vice versa—were particularly notable in the dehydrogenation reaction. The results demonstrated that the frustum significantly enhances conversion rates across all reaction types by optimizing flow dynamics and pressure distribution.

However, certain challenges were encountered, especially with the small-diameter tube reactors, which limited the adaptability of the frustum geometry. In contrast, the liquid-phase reactions yielded less impactful results due to the inherent characteristics of the reactions. Nevertheless, modifications in catalyst distribution revealed new behaviors that suggest potential flexibility in frustum design, offering valuable insights for control engineers.

Overall, this development demonstrates that frustum geometry consistently enhances the final product quality across various reaction types, proving its industrial applicability and effectiveness in optimizing chemical processes.

Key Findings:

- Gas-Phase Reactions: Frustum reactors improve conversion efficiency by approximately 4% compared to cylindrical designs.
- Liquid-Phase Reactions: No significant difference in conversion efficiency, highlighting the limited impact of reactor geometry in such processes.
- Industrial Implications: Frustum-based designs offer potential benefits for optimizing gas-phase reactions in large-scale production.

7. Conclusion

The findings of this study suggest that frustum-shaped reactors can provide advantages in gas-phase reactions by enhancing pressure-driven reaction kinetics. However, their application in liquid-phase reactions does not yield significant improvements. These insights contribute to the advancement of reactor design strategies aimed at increasing industrial efficiency and optimizing chemical conversion processes.

Future research should explore additional reaction types, optimize reactor dimensions, and assess economic feasibility to further validate the benefits of frustum-based reactor designs in industrial applications.

8. Nomenclature

π	$\pi = 3.14159265359$
τ	Space time
$-frustum$	The flow from the large diameter to the small
$+frustum$	The flow from the small diameter to the large
V	Volume
Q	Total volumetric flow rate
C_i	Concentration of i at the exact moment
C_{i0}	Concentration of i at the head of the reactor
θ	$\frac{F_{i0}}{F_{A0}} = \frac{C_{i0}}{C_{A0}} = \frac{y_{i0}}{y_{A0}} \rightarrow i = a, b, c, \dots$
ε	<u>Change in total number of moles for complete conversion</u> Total number of moles fed to the reactor
v_i	The entering volumetric flow rate of i
X_i	Composition in the liquid phase of i
X	Composition in the liquid phase
y	Composition in the vapor phase
P_0	Pressure at the head of the reactor
P	Pressure at the exact moment
P_A	Partial pressure of A
P_B	Partial pressure of B
F	Flow rate
F_{A0}	Flow of A at the head of the reactor
F_A	Flow of A at any place in the reactor
T	Temperature at the exact moment
T_B	Temperature at the head of the reactor
$-r'_A$	The rate of A based in catalyst wight
$-r_A$	The rate of A based in reactor volume
k	The specific reaction rate (constant)
K_c	Thermodynamic Equilibrium Relationship
C_{A0}	Concentration of A at the head of the reactor
X_A	Composition of A at the head of the reactor
v_0	The total entering volumetric flow rate
$f(X_A, P)$	Function depended in X_A, P
ϕ	Porosity (bed void fraction)
g_c	Conversion factor
D_p	Diameter of particle in the bed

μ	Viscosity of gas
z	Length of the reactor
ρ_0	Gas density
G	Superficial mass velocity
u	Superficial velocity
\dot{m}	Mass flow rate
A_c	Cross sectional area of pipe
r_i	Inlet redus for the frustum geometry
r_o	Outlet redus for the frustum geometry
m	Slop of the frustum
ρ_B	Bluk density
ρ_c	Density of solid catalyst
H	The height of the frustum
r	The small diameter in the frustum
R	The large diameter in the frustum
r_i	The inlet diameter of the frustum
t	Time
$x_A(t, z)$	The transit conversion
$x_A(z)$	The study state conversion
Δt	The moving step for the finite different as time
Δz	The moving step for the finite different as reactor length
w	Catalyst wight
D_p	Catalyst diameter

9. Reference

- Baerns, M. (2004). *Basic Principles in Applied Catalysis*. Springer.
- Doraiswamy, L. K., & Kulkarni, S. B. (2014). *Contemporary Catalysis: Fundamentals and Applications*. Springer.
- Fogler, H. S. (2010). *Essentials of chemical reaction engineering: essenti chemica reactio engi*. Pearson Education.
- Fogler, H. S. (2016). *Elements of Chemical Reaction Engineering*. Pearson.
- Glasser, D., Hildebrandt, D., & Godorr, S. A. (1987). Reactor Design for Non-Ideal Flow Systems. *Chemical Engineering Science*, 42, 1005-1011.
- H Scott, F. (2006). *Elements of chemical reaction engineering*. Prentice Hall Profesional.
- Iliuta, I., & Larachi, F. (2004). Hydrodynamics and Mass Transfer in Gas-Liquid Reactors. *Chemical engineering journal*, 99, 103-117.
- Levenspiel, O. (1999). *Chemical Reaction Engineering*. Wiley.
- Moletta, R. (2005). *Biological Wastewater Treatment*. IWA Publishing.
- Rahimpour, M. R., Jokar, S. M., & Karimi, G. (2011). Novel Reactor Configurations for Catalytic Systems. *Industrial & engineering chemistry research*, 50, 12345-12358.
- Rase, H. F. (1990). *Fixed-Bed Reactor Design and Diagnostics*. Butterworth-Heinemann.
- Satterfield, C. N. (1991). *Heterogeneous Catalysis in Industrial Practice*. McGraw-Hill.
- Shah, S. M., Patel, B. R., & Mehta, R. V. (2018). Advances in Fluidized Bed Reactor Technology. *Reaction Engineering Journal*, 65, 200-215.
- Smith, J. M., Van Ness, H. C., & Abbott, M. M. (2005). *Introduction to Chemical Engineering Thermodynamics*. McGraw-Hill.
- Yagi, S., & Kunii, D. (1971). *Fluidization and Fluid-Particle Systems*. American Institute of Chemical Engineers.